

Role of alternative fuels on particulate matter (PM) characteristics and influence of the diesel oxidation catalyst

Fayad, Mohammed; Herreros, Jose; Martos, Francisco; Tsolakis, Athanasios

DOI:

[10.1021/acs.est.5b02447](https://doi.org/10.1021/acs.est.5b02447)

License:

None: All rights reserved

Document Version

Peer reviewed version

Citation for published version (Harvard):

Fayad, M, Herreros, J, Martos, F & Tsolakis, A 2015, 'Role of alternative fuels on particulate matter (PM) characteristics and influence of the diesel oxidation catalyst', *Environmental Science and Technology*, vol. 49, no. 19, pp. 11967–11973. <https://doi.org/10.1021/acs.est.5b02447>

[Link to publication on Research at Birmingham portal](#)

Publisher Rights Statement:

This document is the Accepted Manuscript version of a Published Work that appeared in final form in Environ. Sci. Technol, copyright © American Chemical Society after peer review and technical editing by the publisher.

To access the final edited and published work see <http://dx.doi.org/10.1021/acs.est.5b02447>

See <http://pubs.acs.org/page/policy/articlesonrequest/index.html>.

General rights

Unless a licence is specified above, all rights (including copyright and moral rights) in this document are retained by the authors and/or the copyright holders. The express permission of the copyright holder must be obtained for any use of this material other than for purposes permitted by law.

- Users may freely distribute the URL that is used to identify this publication.
- Users may download and/or print one copy of the publication from the University of Birmingham research portal for the purpose of private study or non-commercial research.
- User may use extracts from the document in line with the concept of 'fair dealing' under the Copyright, Designs and Patents Act 1988 (?)
- Users may not further distribute the material nor use it for the purposes of commercial gain.

Where a licence is displayed above, please note the terms and conditions of the licence govern your use of this document.

When citing, please reference the published version.

Take down policy

While the University of Birmingham exercises care and attention in making items available there are rare occasions when an item has been uploaded in error or has been deemed to be commercially or otherwise sensitive.

If you believe that this is the case for this document, please contact UBIRA@lists.bham.ac.uk providing details and we will remove access to the work immediately and investigate.

The Role of Alternative Fuels on PM Characteristics and Influence of the Diesel Oxidation Catalyst

Mohammed A. Fayad^a, Jose M Herreros^a, Francisco J. Martos^b, and Athanasios Tsolakis^{a*}

^a School of Mechanical Engineering, University of Birmingham, Edgbaston, Birmingham B15 2TT, UK

^b Escuela Técnica Superior de Ingeniería Industrial, University of Málaga, 29071, Málaga, Spain

* Corresponding author. tel.: +44 (0) 121 414 4170, a.tsolakis@bham.ac.uk

Abstract

The influence of a platinum:palladium (Pt:Pd) based diesel oxidation catalyst (DOC) on the engine out particulate matter (PM) emissions morphology and structure from the combustion of alternative fuels including alcohol-diesel blends and rapeseed oil methyl ester (RME) biodiesel was studied. PM size distribution was measured using a scanning mobility particulate spectrometer (SMPS) and the PM morphology and microstructure including size distribution, fractal geometry and number of primary particles was obtained using a high resolution transmission electron microscopy (TEM).

It is concluded that the DOC does not modify the size or the microstructural parameters of the primary particulates that make up the soot agglomerates. The PM reduction seen in the DOC is due to the trapping effect, and oxidation of the PM's volatile components. The DOC performance in reducing gaseous e.g. carbon monoxide (CO), unburnt hydrocarbons (HCs) and PM emissions at low exhaust temperatures was improved from the combustion of alternative fuels due to the reduced level of engine out pollutants.

Keywords: diesel oxidation catalyst, alternative fuels, particulate matter, gaseous emissions.

24 **Introduction**

25 Due to recent popularity of the diesel powered vehicles, the increased particulate matter
26 (PM) emissions have become a major concern to human health and environment.^{1,2} Particulate
27 emissions from compression ignition (CI) engines are variable in size and morphology making
28 their control challenging. Therefore, understanding PM characteristics is likewise necessary for
29 the design of the control technologies like the particle traps. The morphology of the soot particles
30 is characterised by the size and the shape, and quantified by the fractal dimension.^{3,4} The
31 microstructure of the soot primary particulates is quantified by the interlayer spacing (d_{002}) and
32 the thickness (L_c) and width (L_a) of the graphene layer. It is reported that a large interlayer
33 spacing and small graphene layer thickness and width is representative of more disorder soot^{5,6}
34 (which have been seen as an indication of easier soot oxidation).^{7,8} Some studies have reported
35 that there is no direct correlation between the initial (fresh soot) microstructural parameters of
36 soot/PM and its oxidation readiness. This suggests that there are other parameters such as the
37 functional groups present in the soot of the primary particulates that may affect its oxidation
38 characteristics.⁹

39 There are methods to reduce pollutant emission and can be classified into different
40 approaches: improved fuels quality and, use of alternative fuels such as biofuels can
41 enhance/modify the combustion process and reduce the engine out pollutants leading to
42 improved aftertreatment systems (e.g.diesel oxidation catalyst-DOC) performance.¹⁰⁻¹³

43 Alcohol fuels are commonly used in spark ignition engines, but their blends with diesel
44 fuel have also been considered in compression ignition engines and emission benefits have been
45 reported.^{11,13} Some properties of alcohols such as its short chain and oxygen content can provide
46 significant reduction in unburnt hydrocarbons (HCs), PM, and carbon monoxide (CO)
47 emissions.^{14,15} Butanol has been considered as a feasible fuel for use also in diesel engines due to

48 its higher energy density, higher miscibility in diesel fuel and better blending stability than
49 ethanol.^{15,16} A ternary blend alcohol-diesel-biodiesel is considered to compensate for the low
50 cetane number and lubrication properties of the alcohol fuels. On the other hand, the engine
51 performance, exhaust emission, lubricity and fuel miscibility are affected by variation in
52 biodiesel composition in fuel blend.^{17, 18}

53 One of the approaches to meet the emissions regulations is the use of advances aftertreatment
54 units such as selective catalytic reduction (SCR) for the control of NO_x emissions; diesel
55 particulate filters (DPF) to trap PM¹⁹; and DOC to eliminate CO and HC emissions and to
56 generate NO₂ for use in passive regeneration of the DPF and to promote NO_x reduction in the
57 selective catalytic reduction (SCR) systems.¹⁰ There are some exhaust conditions where catalytic
58 reactions can be promoted and inhibited and are dependant on the presence and quantity of
59 different species in the engine exhaust. DOC with high suitable loadings of a catalytic material,
60 such as platinum and high cell density, could also physically trap and oxidise the volatile
61 component of PM.^{11,20,21} Furthermore, the majority of those studies are performed only for
62 conventional diesel fuel²¹⁻²³ and the issues associated to particulate matter oxidation/reduction in
63 the DOC have not been in depth addressed. Therefore, the main objective of this study is to
64 understand the combined effect of the fuel and DOC on the size, morphology and microstructure
65 of the soot agglomerates. The exhaust emission interactions (obstruction/promotion) for CO, HC
66 and NO oxidation on a DOC from the combustion of butanol blends (16 % butanol, 15% RME
67 and 69% diesel), rapeseed oil methyl ester (RME) and diesel fuelling were also investigated.

68 **Experimental set-up and methodology**

69 The schematic diagram of the diesel engine and aftertreatment system set-up is shown in
70 figure S1 (see supporting information). The catalyst activity studies have been carried-out using

71 exhaust from a naturally aspirated single cylinder four stroke, direct injection diesel engine; the
72 main specifications of diesel engine are presented in table S1. Intake air flow, fuel consumption,
73 exhaust pressure and exhaust temperature were also measured.

74 Ultra low sulphur diesel (ULSD) fuel, biodiesel derived from rapeseed oil (RME) fuel
75 used in this study and was supplied by Shell Global Solutions UK. Butanol used in blending with
76 diesel fuel and RME and was purchased from Fisher Scientific. The physical and chemical
77 properties of the pure components were calculated or obtained from provided company or
78 publications (Table 1). This blend was selected due to the favourable fuel blend properties and
79 emissions results when used in compression ignition engines according to Sukjit et al.¹¹ The
80 properties of the fuel blends are presented in Table 1.^{11,18} As shown in Figure S2 (see supporting
81 information), the selected fuel blends tested were B16R15D (16 % butanol, 15% RME and 69%
82 diesel).

83 The DOC used in this research is a 120 g/ft³ Platinum: Palladium (weight ratio 1:1) with
84 alumina and zeolite washcoat (2.6 g/in³ loading) on a cordierite honeycomb monolith. Diameter,
85 length and wall thickness of the DOC are 25.4 mm, 91.4 mm and 4.3 mil respectively with 400
86 cells per in². The DOC used in this study was supplied by Johnson Matthey Plc.

87 Gaseous emissions emitted from the diesel engine such as CO, NO_x, and total
88 hydrocarbons HCs, were measured using a MultiGas 2030 FTIR spectrometry based analyzer. A
89 scanning mobility particle sizer (SMPS) was employed to measure the size of particulate matter
90 emissions emitted from the diesel engine. A model TSI SMPS 3080 particle number and size
91 classifier with thermodiluter was utilized to evaluate the two parameters of the PM emissions
92 which it is the number of concentration and size. The thermodiluter was fitted with air
93 temperature at 150 °C and dilution ratio was set at 1:200 for all tests.

94 The soot particulate samples used in morphology studies have been collected from the
95 exhaust gas stream in different points in 3 mm copper grids attached to a sampling probe. These
96 soot particulates were analysed using a high resolution transmission electron microscopy (HR-
97 TEM) with a Phillips CM-200 microscope which have high resolution about 2 Å at an
98 accelerating voltage of 200 kV. The morphological parameters of the agglomerates (radius of
99 gyration, number of primary particles and fractal dimension) and microstructural parameters
100 (interlayer spacing and thickness of graphene layer) were obtained from the TEM micrographs
101 using a homemade Matlab software (digital image analysis software).^{24, 25}

102 All the tests were carried out in steady state at an engine speed of 1500 rpm with an
103 engine load of 4 bar IMEP representing approximately 45 % of the maximum load. The DOC
104 was loaded inside a furnace to independently study the effects of temperature, space velocity, and
105 exhaust composition and exposed to the engine exhaust keeping a gas space velocity of 35000/h
106 and a heating temperature of about 2 °C/min.

107 **Results and discussions**

108 **DOC effect on Particulate Matter**

109 Particulate matter size distribution and morphology studied from the combustion of the
110 different fuels has been carried out in order to identify the influence of the DOC in the (i)
111 oxidation of gaseous hydrocarbons which can later be nucleate, adsorbed or condensed to form
112 particulate matter, (ii) oxidation or desorption of the hydrocarbon already present onto the
113 particulate matter, (iii) agglomeration of particulates that may lead in increasing the number of
114 particulates and the size of the agglomerates, (iv) trapping effect due to the deposition by
115 diffusion of particulates in the DOC channels and (v) oxidation of soot particulates.

116 The particulate number concentration for diesel fuel combustion is significantly higher
117 for all the particulate sizes compared to RME and the butanol blend combustion as depicted in
118 Figure S3 (see supporting information). This lower particulate number concentration in the case
119 of oxygenated fuels has been previously reported in the literature.²⁶ The oxygen content in the
120 ester group of RME and in the hydroxyl group of butanol are the main reasons to justify the
121 lower engine out PM emissions.

122 Figures 1a & b show the number of particulate matter reduced in the DOC from the
123 combustion of the four fuels when the catalyst inlet temperature is 400 and 500 °C, respectively.
124 For temperatures lower than 400 °C (i.e. 100 °C, 200 °C, 300 °C) the influence of DOC on PM
125 was the same to 400 °C and the results are not shown to avoid duplication. The reduction in the
126 number of particulates in the DOC reaches a constant level around 30% for particulates larger
127 than 50 nm.

128 The average particulate electrical mobility diameter (obtained with the SMPS) and
129 average gyration radius (obtained from the TEM images, Figure S4 included in supporting
130 information) have been compared in Figure 2. Furthermore, the number of primary particulates
131 which compose the aggregates is also plotted in Figure 2. In all the cases (Figure 2) the values of
132 the average mobility diameter and gyration diameter are similar and of the same rank, even
133 though they are based on different measurement methods (e.g. mobility diameter is obtained
134 from particulates after dilution, while TEM analysis is obtained directly from exhaust
135 agglomerates). The average particulate size for butanol blend and RME is lower than in the case
136 of diesel fuel combustion. However, the smaller average agglomerate size of the particulates
137 emitted with RME and the butanol blend is not due to an increase in the number of small
138 particulates but due to a significant reduction in the number of larger ones.^{11,18}

139 There is also an increase in the average particulate size along the catalyst trend that is
140 supported by the mobility diameter (SMPS) and to lesser extent by the radius of gyration results
141 obtained by TEM. This increase is obtained at both 400 and 500 °C temperatures for all the
142 studied fuels. This increase in the mean particulate diameter is due to the higher diffusion losses
143 associated to the particulates of smaller diameters (below 20 nm) as well as due to the collision
144 of particulates in the DOC channels. This leads to the formation of larger size agglomerate from
145 the high number of primary particles as it was also confirmed from the TEM results (Figure 2).
146 The trapping effect of the small particulates is the major effect in the exhaust gas from the
147 combustion RME and butanol blends as the agglomerates analysed with TEM upstream and
148 downstream the catalyst have similar size (Figure 2). However, the increase in the agglomerate
149 size in the case of diesel fuel is dominated by the collision and further aggregation between them
150 as it is shown in the TEM results (Figure 2). The higher number of particulates in the case of
151 diesel fuel combustion increases the likelihood of collisions between them. The larger reduction
152 in the number of particulate matter when the DOC temperature is 500 °C with respect to 400 °C
153 in the case of RME cannot be due to the oxidation of gas phase hydrocarbon as the DOC
154 oxidation efficiency was the same for both temperatures. It could be interpreted as an indication
155 of the oxidation of organic material already contained in the particulates or an indication of soot
156 oxidation activity due to the lower soot oxidation temperature from RME combustion as it has
157 been previously reported.^{26,27} This should be confirmed by the morphological and
158 microstructural results discussed below.

159 The fractal dimension (D_f) obtained for all the conditions are in the typical range of
160 diesel particulates (1.7-1.8) which is characteristic of diffusion limited aggregation
161 mechanism growth.²⁸ According to the results, the fractal dimension of the aggregates of

162 particulates produced from the combustion of diesel fuel is larger than those produced from the
163 combustion of RME, and the butanol blend (Figure 3). Soot aggregates from the diesel fuel
164 combustion have a more pronounced spherical shape compared to the rest of the fuels.^{24,28}
165 Therefore, it is expected that the particulates emitted from the alternative fuels to be easier to be
166 trapped in the filters due to their chain shape morphology.

167 The PM shape was also changed over the DOC due to the aggregation as well as thermal
168 restructuring of the agglomerates due to the temperature increase within the catalyst. As a
169 result, the particles downstream the DOC have slightly more spherical shape, especially in the
170 case of those emitted from diesel fuel. It can be noted that the DOC has considerable reduction
171 and a significant influence on the size and concentration of particulate emissions, which in turn
172 enables to reduce tail pipe PM emission.

173 The size of primary particulates (d_{p0}) and the microstructural parameters for all the
174 studied fuels has also been investigated and presented in Figure S5 (see supporting
175 information). A statistically significant number of primary particulates (around 150-200)
176 for each fuel and condition (before and after the DOC) has been measured to produce the
177 fitted lognormal/normal distribution (Figure S5 included in supporting information) and
178 calculate the mean primary particulate size (Figure 4). It can be obtained that the size of
179 primary particulates is bigger in the case of diesel fuel combustion, while the smallest
180 primary particulates size are obtained from the combustion of butanol blend. This is a
181 result of the lower rate of production of soot precursors, which limits the soot formation
182 and increases the soot oxidation rate during the combustion process of the oxygenated
183 fuels. This result together with the morphology results demonstrates that the smaller size
184 agglomerates in the case of oxygenated fuels is due to the lower number of primary

185 particulates as well as the smaller size of the primary particulates which composed the
186 agglomerates. It can also be concluded that the DOC does not modify the primary
187 particulate size in any of the fuels. This result supports the idea that the DOC only affects
188 the particulate agglomerates rather than the primary particulates which would need higher
189 temperatures and residence time in the catalyst to be oxidised.

190 PM microstructure (Figure 5) has been quantified by the average interlayer spacing
191 (d_{002}) and average thickness of the graphene layer which composed the soot primary
192 particulates. It is shown that the interlayer spacing from the soot produced from RME and
193 butanol blends combustion is smaller than those found in the soot produced from diesel
194 combustion (Figure 5). However, there are no statistical significant differences between the
195 average thicknesses of the graphene layer derived from the combustion of the studied
196 fuels. The smaller interlayer spacing for the soot derived from oxygenated fuels is an
197 indication of a more ordered structure being supported by the literature.¹⁰ Figure 5 also
198 shows that the DOC does not produce any statistical significant effect to the microstructural
199 parameters obtained from the PM of all the fuels.

200 Based on the morphology and microstructural results of particulate matter
201 upstream and downstream the diesel oxidation catalyst, it can be concluded that DOC
202 oxidises the adsorbed hydrocarbons on PM (effect ii), leads to agglomeration of
203 particulates (effect iii) and traps by diffusion some of the solid particulates (effect iv).
204 However, the DOC it is not able to oxidise the soot (effect v). It is proposed that the
205 residence time between the soot and the catalysed active sites within the DOC is not
206 enough to oxidise it irrespective of the fuel used.

217 **CO reduction in the DOC**

218 The CO and HCs engine output emissions from the combustion of conventional diesel
219 fuel are higher compared to the rest of the tested fuels (Figure S6 included in supporting
220 information). The high level of CO and HCs for diesel combustion hampers the CO adsorption
221 onto the catalyst (zeolites) at low exhaust gas temperatures.¹⁰ leading to a delay in the start of CO
222 light-off compared to the other fuels (Figure 6). On the contrary, the lower engine output HC and
223 CO concentration from the combustion of RME and alcohol blend (Figure S6 included in
224 supporting information) reduces the possibility for obstruction from CO and HC competition and
225 improved the catalyst CO light-off. At low temperatures, the CO oxidation in the DOC is
226 kinetically limited (poor accessibility to active sites by other component inhibition).²⁹

227 Once the oxidation has started, there are some plateaus in the CO light-off curves for
228 most of the fuels (around 100-150 °C). At high exhaust temperatures, CO is not
229 thermodynamically limited and the heat release from its oxidation increases the local temperature
230 of the catalyst. This higher active site temperature helps the oxidation of CO (Figure 6),
231 especially in the case of diesel fuel combustion where the level of CO emission is higher.
232 Moreover, this higher rate of CO oxidation for the case of diesel fuel at this temperature could be
233 due to high hydrocarbon depletion as shown in Figure 7. At higher temperatures (approximately
234 180 °C), the CO oxidation in the DOC catalyst for diesel combustion reaches 100 % at lower
235 temperature compares to the rest of the fuels, especially for RME (Figure 6). The exhaust from
236 the RME combustion has the lowest level of CO and the highest levels of NO_x leading to
237 reduced exothermic and increased competition for active sites between CO and NO.²³

228 **HC's reduction in the DOC**

229 The low temperature hydrocarbon conversion seen in the DOC is due to the trapping
230 effect by the zeolites ('virtual conversion').²³ When temperature increases and the

231 conversion efficiency for CO is high; the catalyst active sites become available for HCs
232 adsorption and oxidation. It can be seen that HCs oxidation for all the fuels increased once
233 CO was fully oxidised (Figure 6 and Figure 7).

234 The lowest HCs conversion efficiency over the DOC occurs for the case of diesel fuel
235 combustion. This is due to the higher upstream concentration of engine out aromatic
236 hydrocarbons which have been reported to be more difficult to be adsorbed and oxidised.^{18,}
237 ^{22, 30, 31} Meanwhile, higher HC conversion in the DOC noted when exhaust gas from the
238 combustion of the RME was used and this is due to the absence of aromatic hydrocarbons
239 in the fuel structure. Moderate HC conversion is obtained when exhaust gas from for the
240 combustion alcohol blends was used and this is due to the large presence of diesel in the
241 fuel blend, partially compensated by the presence of the alcohol.

242 **NO to NO₂ oxidation in the DOC**

243 The oxidation of NO to produce NO₂ in the DOC (Figure 8) is influenced by the
244 different concentrations of CO, NO and by the concentration and type of HCs. It can be
245 observed that at low temperature the NO₂ concentration downstream the DOC is lower
246 than the engine output NO₂. This is the effect of NO₂ reacting with CO and HC in the DOC
247 catalyst.

248 The increase in the NO₂ concentration downstream the catalyst starts around the
249 same temperatures (approximately 220 °C) for all the studied cases, once the CO has been
250 completed oxidised by oxygen in the catalyst active sites. Hence, it is evident the inhibition
251 of CO on NO₂ production occupying the catalyst active sites as well as the consumption of
252 any NO₂ created by reaction with CO and HCs to form CO₂.

253 It is noticeable the higher NO₂ concentration downstream the catalyst at
254 temperatures below 350 °C was seen in the case of butanol combustion. The formation of
255 some very active oxygenated hydrocarbon components which could be formed in the
256 catalyst can enhance NO₂ production. A similar effect has been already reported in the case
257 of Ag/Al₂O₃ catalyst where the formation of NO₂ is highly promoted under the addition of
258 alcohol fuels.^{32,33} At temperatures higher than 350 °C the NO₂ production is not further
259 increasing forming a plateau as the NO₂ production from NO oxidation is thermodynamic
260 limited.³⁴

261 **Influence of DOC technology on PM emissions from the combustion of alternative fuels**

262 The purpose of the present work was to investigate the effects of a diesel oxidation
263 catalyst on particulate matter characteristics and gaseous emissions from the combustion of
264 alternative fuels. This study gives an insight regarding of the effects of alternative fuels on the
265 DOC performance over (i) particulate matter reduction/modification, (ii) pollutant emissions
266 oxidation such as CO and THCs to CO₂ and H₂O and (iii) NO oxidation to NO₂ which can be
267 further used in the catalytically reduction of NO_x in the SCR or in the DPFs for passive
268 regeneration.

269 The combustion of alternative fuels produces lower emissions of unburnt hydrocarbons,
270 CO and PM number concentration which enhances the catalyst activity at lower temperatures by
271 limiting the CO and HCs inhibition effect and DOC performance in long term operation by
272 reducing the PM accumulation effect. PM agglomerates and their primary particles emitted from
273 the combustion of alternative fuels are in average smaller and with a lower fractal dimension,
274 thus are being easier to be trapped or oxidised. It has to be noticed that the average smaller size
275 of the agglomerates emitted from the combustion of alternative fuels is due to the production of

276 lower number of large particulates rather than a high number of small particulates not being
277 detrimental for the environment and/or downstream diesel particulate filter.

278 SMPS and TEM analysis revealed that the PM filtration efficiency in the DOC is higher
279 for the small particles and that there is a PM aggregation process that takes place within the
280 DOC. Furthermore, the DOC does not modify the primary particulates size and microstructural
281 parameters for any of the studied fuels. Therefore, it is thought that the DOC only has a trapping
282 effect on soot and oxidises the PM volatile components, while a longer residence time is needed
283 to oxidise the soot.

284 **Acknowledgements**

285 The Iraqi Government and University of Technology in Baghdad is gratefully acknowledged for
286 the PhD scholarship and maintenance grant for Mr. Mohammed Fayad. Innovative UK (The
287 Technology Strategy Board, TSB) and EPSRC for supporting this work with the projects
288 (CREO: ref. 400176/149) and (EP/G038139/1), respectively. F.J. Martos expresses thanks to the
289 University of Malaga for supporting his research stay at the University of Birmingham. With
290 thanks to Advantage West Midlands and the European Regional Development Fund, funders of
291 the Science City Research Alliance Energy Efficiency project – a collaboration between the
292 Universities of Birmingham and Warwick.

293 **ASSOCIATED CONTENT**

294 Supporting Information

295 Figure S1 shows the simplified schematic diagram of engine and DOC system, while Figure S2
296 shows the ternary diagrams representing the fuel test blends. Figure S3 shows the engine output
297 particulate size distribution for different fuels upstream the diesel oxidation catalyst. TEM and

298 HR-TEM micrographs of particulates matter are shown in Figure S4 and Figure S5, respectively.
299 Engine output gaseous emissions for the different studied fuels are depicted in Figure S6. Table
300 S1 shows the engine specifications. This information is available free of charge via the Internet
301 at <http://pubs.acs.org>.

302 **ABBREVIATIONS**

303 B16R15D = butanol 16 %, RME 15% and Diesel 69%

304 CI = compression ignition

305 CO = carbon monoxide

306 CO₂ = carbon dioxide

307 d₀₀₂ = interlayer spacing

308 DOC = diesel oxidation catalyst

309 D_f = fractal dimension

310 DPF = diesel particulate filter

311 HC = hydrocarbons

312 IMEP = indicated mean effective pressure

313 L_c = graphene layer thickness

314 NO = nitric oxide

315 NO₂ = nitrogen dioxide

316 NO_x = nitrogen oxides

317 n_{po} = number of primary particles

318 R_g = gyration radius

319 RME = rapeseed oil methyl ester

320 SCR = selective catalytic reduction

321 SMPS = scanning mobility particle sizer

322 PM = particulate matter

323 TEM = transmission electron microscopy

324 THC = total hydrocarbons

325 ULSD = ultra low sulfur diesel

326

327 **References**

- 328 [1] Diesel Engine Exhaust Carcinogenic, Press release no. 213; International Agency for
329 Research on Cancer, **2012**; http://www.iarc.fr/en/media-centre/pr/2012/pdfs/pr213_E.pdf.
- 330 [2] Geller, M. D.; Sardar, S. B.; Phuleria, H.; Fine, P. M.; Sioutas, C. Measurements of
331 particle number and mass concentrations and size distributions in a tunnel environment.
332 *Environ. Sci. Technol.* **2005**, 39 (22), 8653-8663.
- 333 [3] Kimijima T.; Haneishi T.; Okabe H. Effect of soot on anti-wear properties of marine
334 diesel engine oils. *J Jpn Soc Tribologis.* **1994**, 39, 337- 344.
- 335 [4] Meakin, P.; Donn, B; and Mulholland, G.W. ‘Collisions between point masses and fractal
336 aggregates’, *Langmuir.* **1989**, 5, 510-518.
- 337 [5] Ishiguro, T.; Suzuki, N.; Fujitani, Y.; Morimoto, H. Microstructural changes of diesel
338 soot during oxidation. *Combust Flame.* **1991**, 85, 1-6.
- 339 [6] Liati, A.; Eggenschwiler, P. D. Characterization of particulate matter deposited in diesel
340 particulate filters: visual and analytical approach in macro-, micro- and nano scales.
341 *Combust Flame.* **2010**, 157, 1658-1670.
- 342 [7] Su, D.S.; Jentoft, R.E.; Müller, J. O.; Rothe, D.; Jacob, E.; Simpson, C.D.; Tomovic, Z.;
343 Müllen, K.; Messerer, A.; Pöschl, U.; Niessner, R.; Schlögl, R. Microstructure and
344 oxidation behaviour of Euro IV diesel engine soot: a comparative study with synthetic
345 model soot substances. *Catal Today.* **2004**, 90, 127-132.
- 346 [8] Vander, Wal, R.; Tomasek, A.J. Soot nanostructure: dependence upon synthesis
347 conditions. *Combust Flame.* **2004**, 136, 129-140.
- 348 [9] Al-Qurashi, K.; Boehman, A. L. Impact of exhaust gas recirculation (EGR) on the
349 oxidative reactivity of diesel engine soot. *Combust Flame.* **2008**, 155, 675-695.
- 350 [10] Lefort, I.; Herreros, JM.; Tsolakis, A. Reduction of low temperature engine pollutants by
351 understanding the exhaust species interactions in a diesel oxidation catalyst. *Environ. Sci.*
352 *Technol.* **2014**, 48, 2361-2367.
- 353 [11] Sukjit, E.; Herreros, J. M.; Dearn, K. D.; García-Contreras, R.; Tsolakis, A. The effect of
354 the addition of individual methyl esters on the combustion and emissions of ethanol and
355 butanol-diesel blends. *Energy.* **2012**, 42 (1), 364-374.
- 356 [12] Choi, B.; Jiang, X. Individual hydrocarbons and particulate matter emission from
357 a turbocharged CRDI diesel engine fuelled with n-butanol/diesel blends. *Fuel.* **2015**,
358 154, 188-195.
- 359 [13] Gunfeel, M.; Yonggyu, L.; Kyonam, C.; Dongsoo, J. Emission characteristics of diesel,
360 gas to liquid, and biodiesel-blended fuels in a diesel engine for passenger cars. *Fuel.*
361 **2010**, 89 (12), 3840-3846.
- 362 [14] Zhang, Z, H.; Balasubramanian, R. Effects of oxygenated fuel blends on
363 carbonaceous particulate composition and particle size distributions from a stationary
364 diesel engine. *Fuel.* **2015**, 141, 1-8.
- 365 [15] Rakopoulos, D. C.; Rakopoulos, C. D.; Papagiannakis, R. G.; Kyritsis, D. C. Combustion
366 heat release analysis of ethanol or nbutanol diesel fuel blends in heavy-duty DI diesel
367 engine. *Fuel.* **2011**, 90 (5), 1855-1867.

- 368 [16] Octavio Armas, O.; García-Contreras, R.; Ramos, A. Pollutant emissions from engine
369 starting with ethanol and butanol diesel blends. *Fuel Process Technol.* **2012**, (100) 63-72.
- 370 [17] Selvan, T ; Nagarajan, G. Combustion and Emission Characteristics of a Diesel Engine
371 Fuelled with Biodiesel Having Varying Saturated Fatty Acid Composition. *Int J Green*
372 *Energy.* **2013**, 10 (9), 952-965.
- 373 [18] Hueseyin, A.; Cumali, I. Effect of ethanol blending with biodiesel on engine performance
374 and exhaust emissions in a CI engine. *Appl Therm Eng.* **2010**, 30 (10), 1199-1204.
- 375 [19] Herner, J. D.; Hu, S.; Robertson, W. H.; Huai, T.; Collins, J. F.; Dwyer, H.; Ayala, A.
376 Effect of Advanced Aftertreatment for PM and NO_x Control on Heavy-Duty Diesel
377 Truck Emissions. *Environ. Sci. Technol.* **2009**, 43 (15), 5928-5933.
- 378 [20] Katare, SR.; Laing, PM. Hydrogen in diesel exhaust: effect on diesel oxidation catalyst
379 flow reactor experiments and model predictions. *SAE Paper.* **2009**, 2009-01-1268.
- 380 [21] Ko, A.; Kim, J.; Choi, K.; et al. Experimental study of particle emission characteristics of
381 a heavy-duty diesel engine and effects of aftertreatment systems: Selective catalytic
382 reduction, diesel particulate filter, and diesel particulate and NO_x reduction. *J. Aut. Eng.*
383 **2012**; 226 (12), 1689-1696.
- 384 [22] Katare, S.; Patterson, J.; Laing, P. Aged DOC is a Net Consumer of NO₂: Analyses of
385 Vehicle, Engine-dynamometer and Reactor Data. *SAE Paper* **2007**, 2007-01-3984.
- 386 [23] Lafossas, F.; Matsuda, Y.; Mohammadi, A.; Morishima, A.; Inoue, M.; Kalogirou, M.;
387 Koltsakis, G.; Samaras, Z. Calibration and validation of a diesel oxidation catalyst model:
388 From synthetic gas testing to driving cycle applications. *SAE Int. J. Engines.* **2011**, 4 (1),
389 1586-1606.
- 390 [24] Lapuerta, M.; Ballesteros, R.; Martos, F. J. A method to determine the fractal dimension
391 of diesel soot agglomerates. *J Colloid Interf Sci.* **2006**, 303, 149-158.
- 392 [25] Lapuerta M.; Martos F.J.; Martín-González G. Geometrical determination of the
393 lacunarity of agglomerates with integer fractal dimension. *J Colloid Interf Sci.* **2010**, 346,
394 23-31.
- 395 [26] Song, J.; Alam, M.; Boehman, A. L.; Kim, U. Examination of the oxidation behaviour of
396 biodiesel soot. *Combust. Flame.* **2006**, 146, 589-604.
- 397 [27] Boehman, A. L.; Song, J.; & Alam, M. "Impact of Biodiesel Blending on Biodiesel Soot
398 and the Regeneration of Particulate Filters", *Energy Fuels.* **2005**, 1857-1864.
- 399 [28] Meakin, P.: In "On growth and Form," edited by Stanley and Ostrowsky, Martinus-
400 Nijhoff Publishers, Boston. **1986**, 111-135.
- 401 [29] Stevanovic, S.; Miljevic, B.; Surawski, N. C.; Fairfull-Smith, K. E.; Bottle, S. E.; Brown,
402 R.; and Ristovski, Z. D. Influence of Oxygenated Organic Aerosols (OOAs) on the
403 Oxidative Potential of Diesel and Biodiesel Particulate Matter. *Environ. Sci. Technol.*
404 **2013**, 47 (14), 7655-7662.
- 405 [30] Hori, M. Experimental study of nitrogen dioxide formation in combustion systems. *Symp*
406 *(Int) Combust.* **1988**, 21(1), 1181-1188.

- 407 [31] Ladommatos, N.; Abdelhalim, S. M.; Zhao, H. Effects of exhaust gas recirculation
408 temperature on diesel engine combustion and emissions. *Proc. Inst. Mech. Eng. J. Aut.*
409 *Eng.* **1998**, 212 (6), 479-500.
- 410 [32] Herreros, J. M.; George, P.; Umar, M.; Tsolakis, A. Enhancing selective catalytic
411 reduction of NO_x with alternative reactants/promoters. *Chem. Eng. J.* **2014**, 252, 47-54.
- 412 [33] Johnson, W.L.; Fisher, G.B.; Toops, T.J. Mechanistic investigation of ethanol SCR of
413 NO_x over Ag/Al₂O₃, *Catal. Today.* **2012**, 184 (1), 166-177.
- 414 [34] Cooper, B.; and Thoss, J. "Role of NO in Diesel Particulate Emission Control," *SAE*
415 *Technical Paper.* **1989**, 890404.

416 **Tables Caption**

417 **Table 1.** Specification of tested fuels [11, 18].

418

Table 1.

Properties	ULSD 100%	RME 100%	Butanol	B16R15D (butanol blend)
Chemical formula	$C_{14}H_{26.1}$	$C_{19}H_{35.3}O_2$	C_4H_9OH	$C_{11}H_{21.4}O_{0.5}$
Cetane number	53.9	54.74	17	
Latent heat of vaporization (kJ/kg)	243	216	58	
bulk modulus (MPa)	1410	1553	1500	
density at 15 °C (kg/m ³)	827.1	883.7	809.5	835.2
kinematic viscosity at 40 °C (cSt)	2.70	4.53	2.23	2.54
lower calorific value (MJ/kg)	43.11	37.80	33.12	39.97
lubricity at 60 °C(μm)	312	205	620	405
C (wt %)	86.44	77.09	64.78	81.56
H (wt %)	13.56	12.07	13.63	13.34
O (wt %)	0	10.84	21.59	5.08
O from OH group (wt %)	0	0	21.59	3.36
Boling point (°C)	-	-	117.5	
50% distillation (°C)	264	335	117	
90% distillation (°C)	329	342	117	

Figures Caption

Figure 1. Particulate matter reduction in the DOC for different fuels for (a) 400 °C, (b) 500 °C.

Figure 2. Particle size of SMPS results Vs. Gyration radius (R_g) and number of primary particles (n_{po}) for (a) diesel fuel, (b) butanol blend (c) RME.

Figure 3. Fractal dimensions of particulates matter from TEM for all fuel tested.

Figure 4. Size of primary particulate (d_{po}) for all fuel tested.

Figure 5. Particulate matter microstructure, high resolution TEM micrograph, interlayer spacing (d_{002}) and graphene layer thickness (L_c).

Figure 6. CO light-off curves from exhaust gas produced for different fuels.

Figure 7. DOC conversion efficiency for THC.

Figure 8. NO and NO₂ catalyst outlet concentration from engine operation.

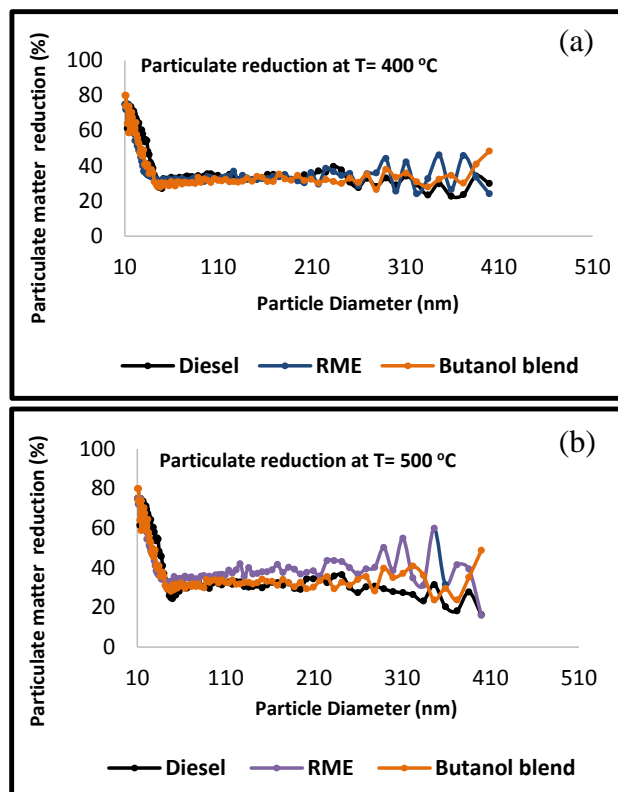


Figure 1.

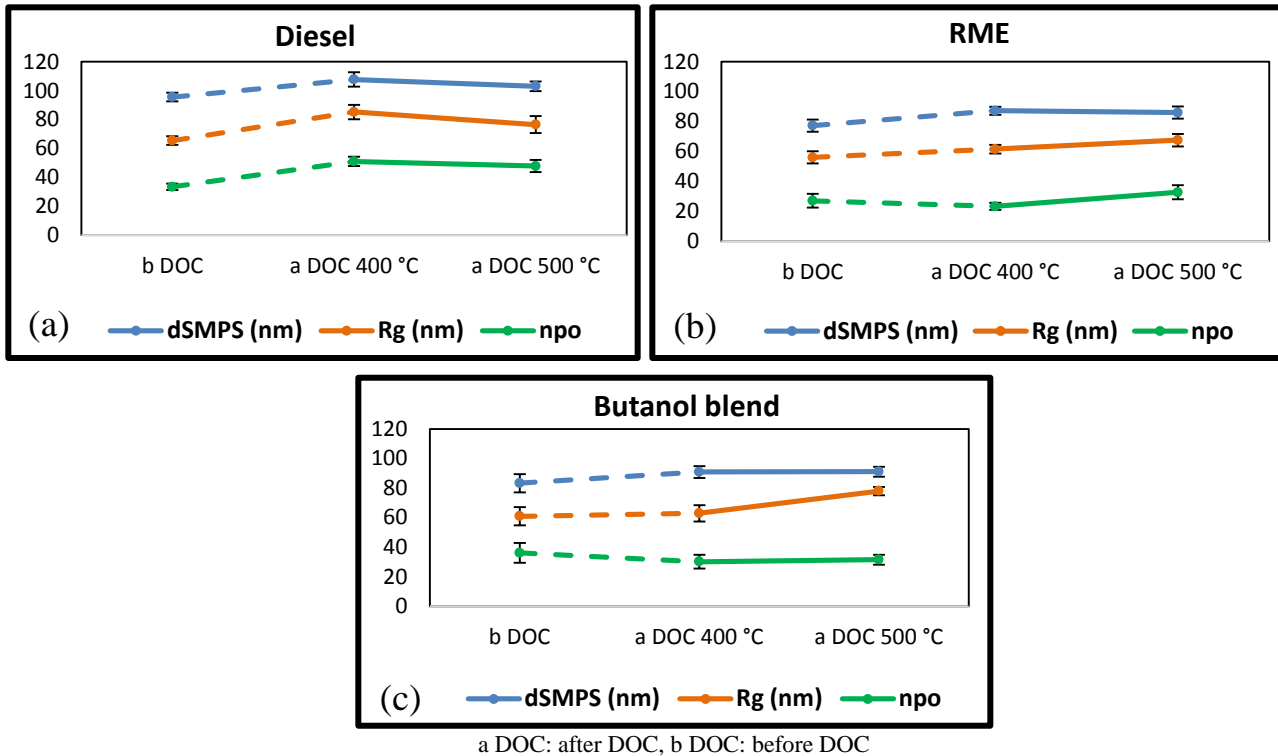


Figure 2.

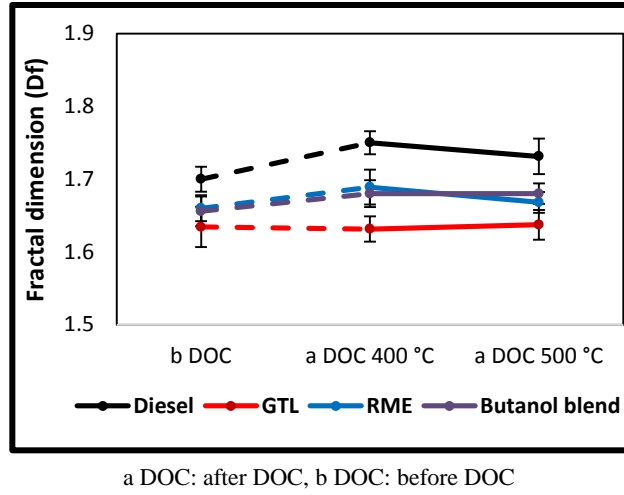
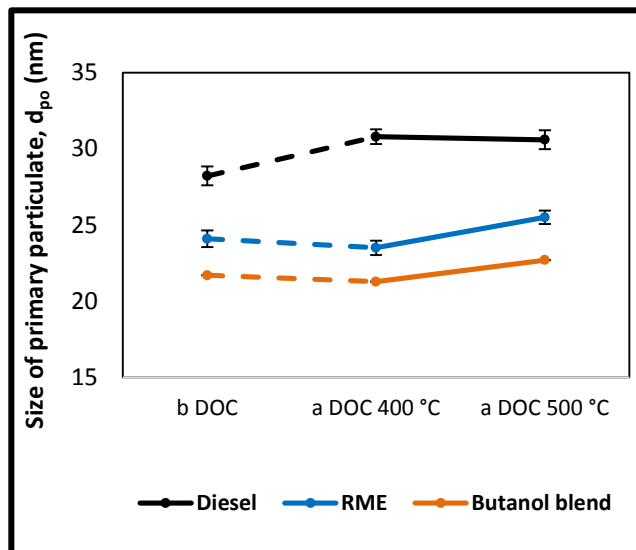
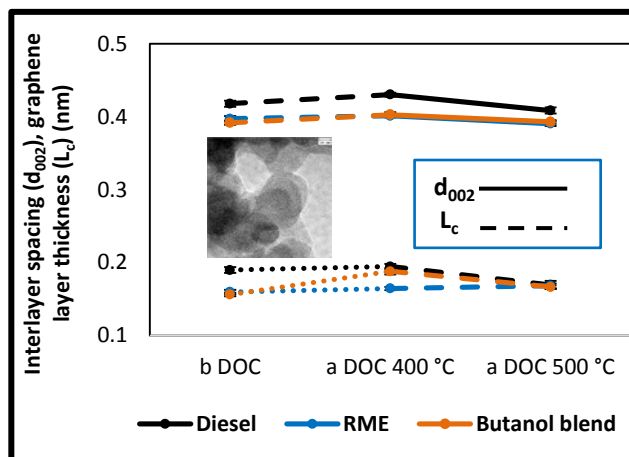


Figure 3.



a DOC: after DOC, b DOC: before DOC

Figure 4.



a DOC: after DOC, b DOC: before DOC

Figure 5.

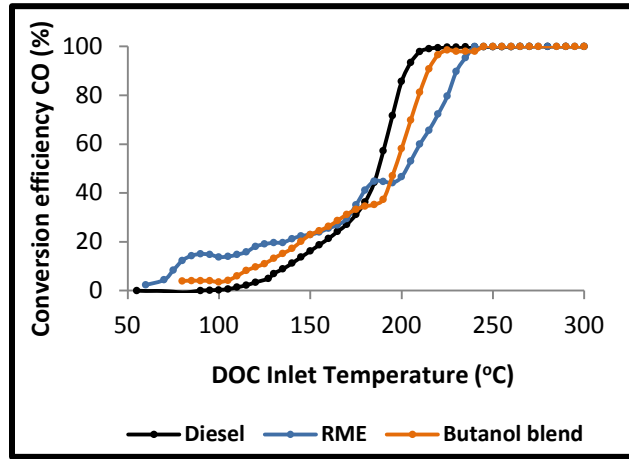


Figure 6.

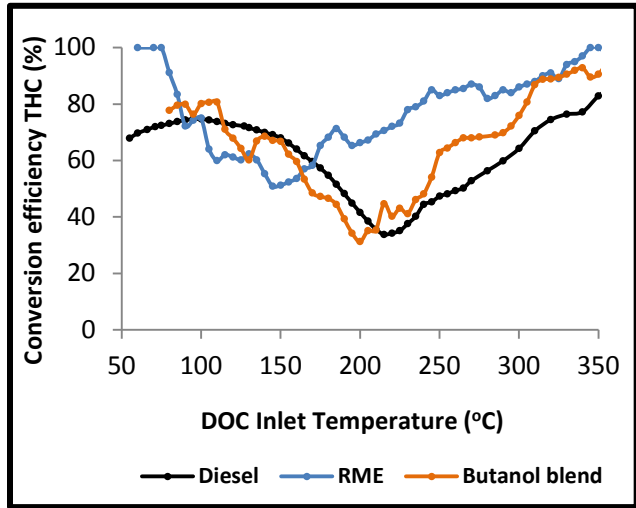


Figure 7.

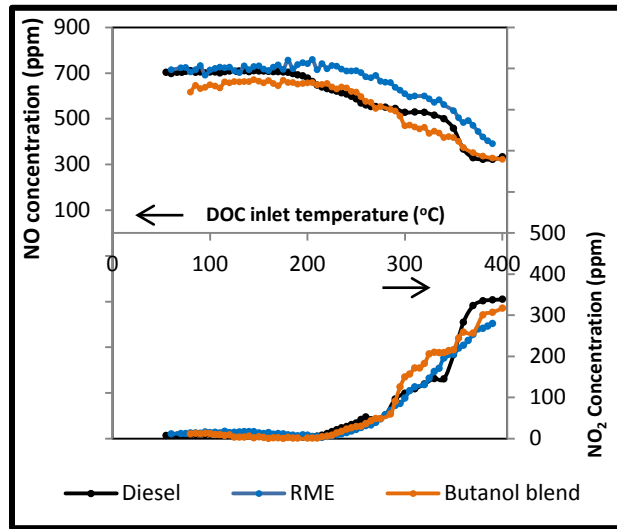


Figure 8.

TOC/Abstract art

